

Supplementary materials

Dual-function sensors based on carbon dots derived from corncob for methyl nicotinate detection in solution and vapor phases

Preeyanuch Supchocksoonthorn,^a Ma Concepcion Alviar Sinoy,^b Sumana Kladsomboon,^c Mark

Daniel G. de Luna,^b Xiao Liang,^d Shufeng Song,^e Peerasak Paoprasert^{a*}

^a*Department of Chemistry, Faculty of Science and Technology, Thammasat University, Pathumthani
12120 Thailand*

^b*Department of Chemical Engineering, University of the Philippines, Diliman, 1101, Quezon City,
Philippines*

^c*Department of Radiological Technology, Faculty of Medical Technology, Mahidol University,
Bangkok, 73170 Thailand*

^d*College of Chemistry and Chemical Engineering, Hunan University, Changsha, Hunan 410082, P. R.
China*

^e*College of Aerospace Engineering, Chongqing University, Chongqing 400044, China*

**Corresponding author, E-mail address: peerasak@tu.ac.th (Peerasak Paoprasert)*

Materials and chemicals

All chemicals used were at least of analytical reagent grade. Quinine sulfate and hydrochloric acid (HCl) were purchased from Acros Organics. LiNO_3 , $\text{Ca}(\text{NO}_3)_2$, Li_2SO_4 , Na_2SO_4 , KCl, MgCl_2 , ZnCl_2 , glucose, fructose, sucrose, urea, alanine, glycine, lysine, human serum (male AB plasma), artificial saliva, methyl phenylacetate, methyl *p*-anisate, *o*-phenyl anisole, MN, 4-vinylpyridine, and pyridine were bought from Merck. Acetonitrile (HPLC grade, Carlo Erba) was used as the mobile phase for HPLC. Artificial urine was purchased from Fortune Scientific Co., Ltd. A dialysis membrane (molecular weight cut-off, MWCO = 1,000 Da), was purchased from Membrane Filtration Products, Inc. Deionized (DI) water (resistivity > 18 $\text{M}\Omega\cdot\text{cm}$) was used in all experiments.

Characterization of CDs

The chemical composition of the CDs was investigated using a Fourier-transform infrared (FT-IR) spectrometer (Perkin Elmer, Spectrum 2000) and an X-ray photoelectron spectrometer (XPS; AXIS ULTRA^{DLD}, Kratos Analytical, Manchester, UK). Size and morphology were evaluated using a JEOL JEM-2100 transmission electron microscope (TEM) with an accelerating voltage of 200 kV at a magnification of 100,000X. The optical absorbance and photoluminescence emission spectra were measured using a Duetta fluorescence and absorbance spectrometer (HORIBA). The HPLC method (Shimadzu, LC-20AT series) was performed using the UV detector (268 nm) and a C18 column joined with a guard column. The validity of the results was evaluated using the *t*-test and *F*-test. A mobile phase of acetonitrile/water (1:1 v/v) was used in a 10- μL injection loop with a flow rate of 1.0 $\text{mL}\cdot\text{min}^{-1}$.

The quantum yields of the CDs were measured based on previous studies^{1, 2}. Briefly, quinine sulfate in 0.1 M H_2SO_4 was used as a reference. The optical absorbance and fluorescence emission areas of the CDs and quinine sulfate at different concentrations were measured (quantum yield = 54%, an excitation at 349 nm). The quantum yield of the CDs was calculated using the slope method.

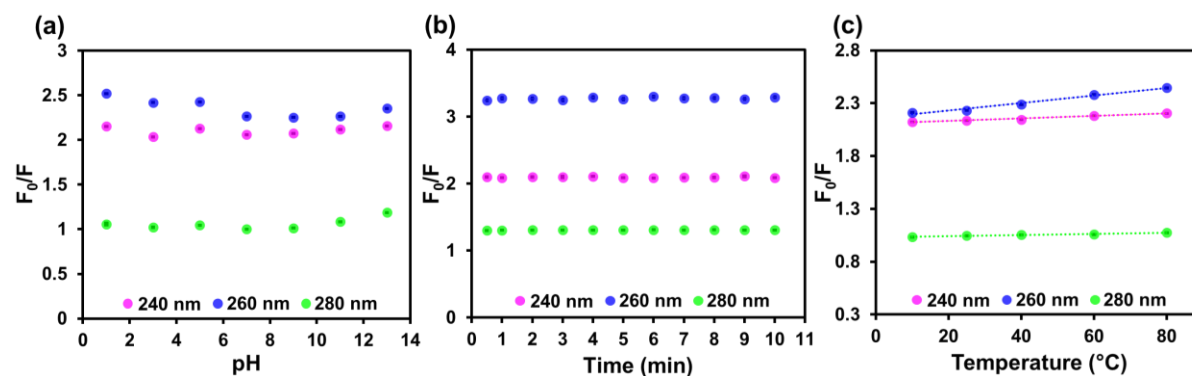


Figure S1. (a) Plot of ratio of fluorescence intensities versus pH, (b) mixing time, and (c) temperature.

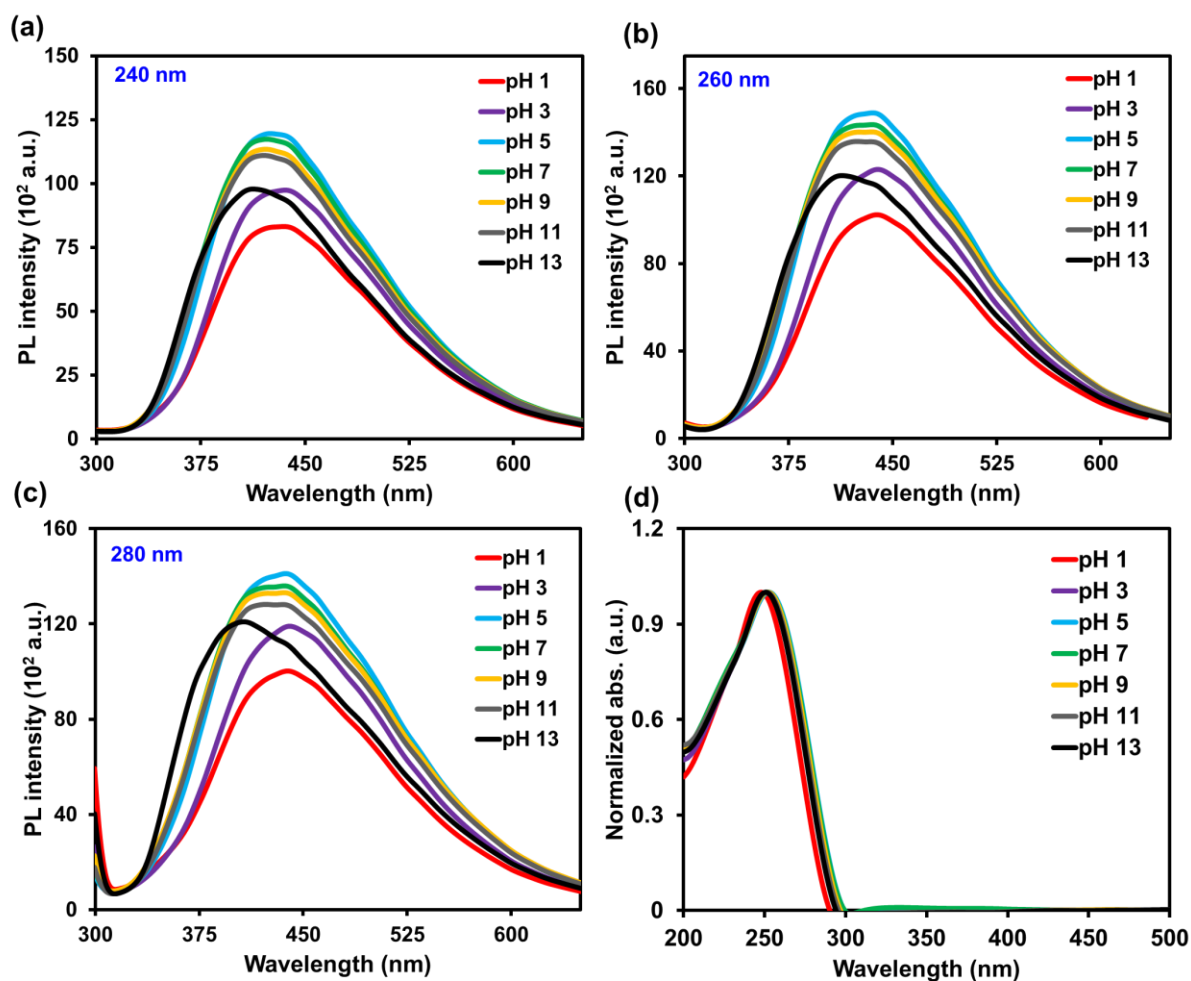


Figure S2. (a-c) Fluorescence emission spectra of carbon dots under different excitation wavelengths (240, 260, and 280 nm) and (d) UV-vis spectra of MN from pH 1 to 13.

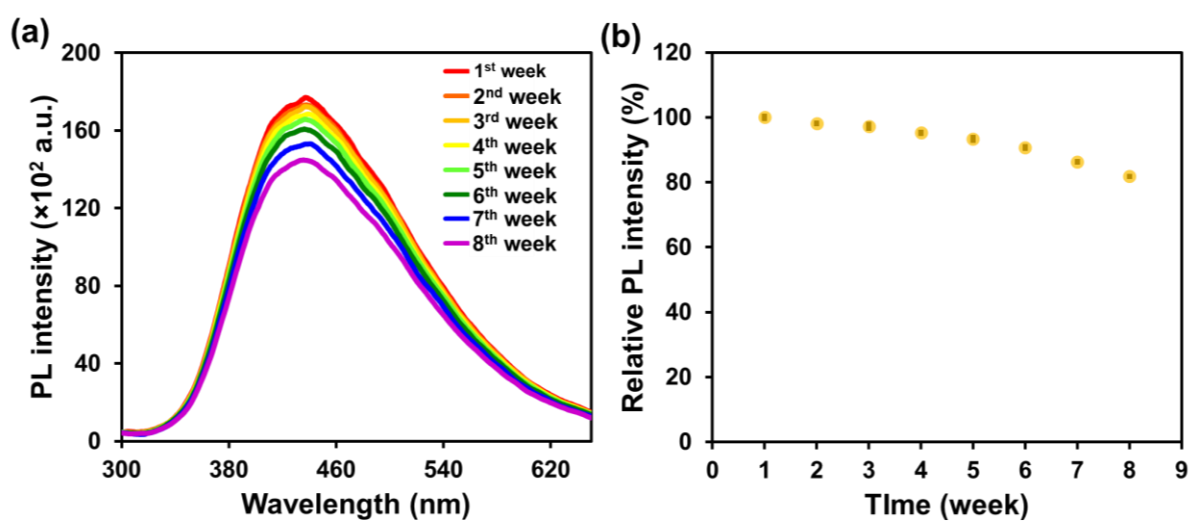


Figure S3. (a) Fluorescence emission spectra of carbon dots using an excitation of 260 nm at different time intervals. (b) Relative fluorescence intensity versus time.

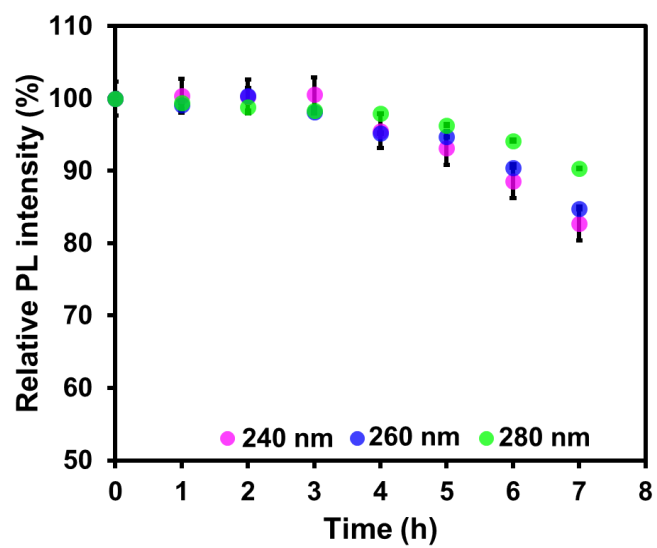


Figure S4. (a) Plot of fluorescence intensities measured at 432 nm and excited at 240, 260, and 280 nm under continuous 365-nm UV irradiation as a function of time.

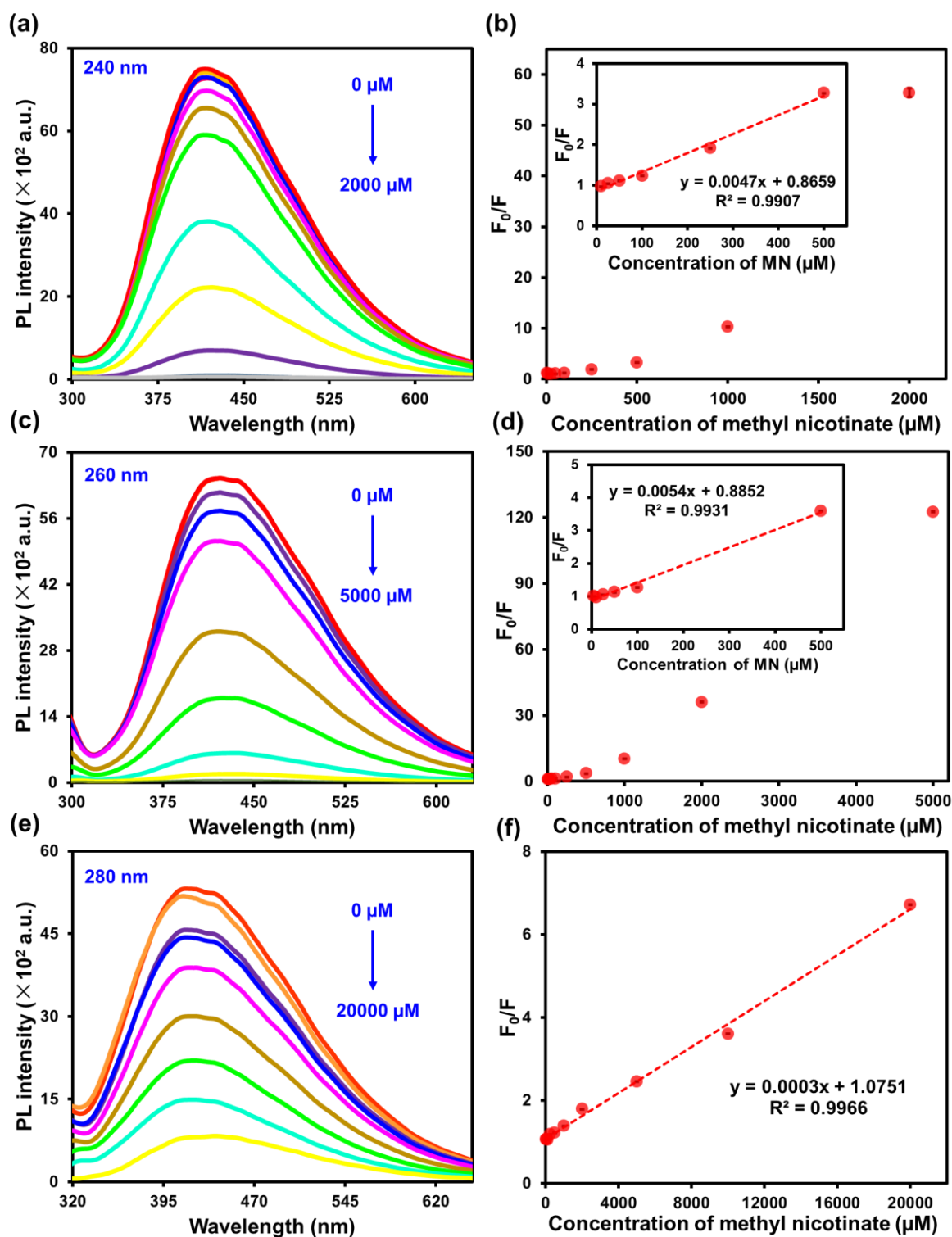


Figure S5. (a, c, e) Fluorescence emission spectra of carbon dots (0.01 mg·mL⁻¹) in the presence of different concentrations of MN at pH 7 with different excitation wavelengths. (b, d, f) The plot between F_0/F and concentrations of MN; inset figure shows the linear range of the plot.

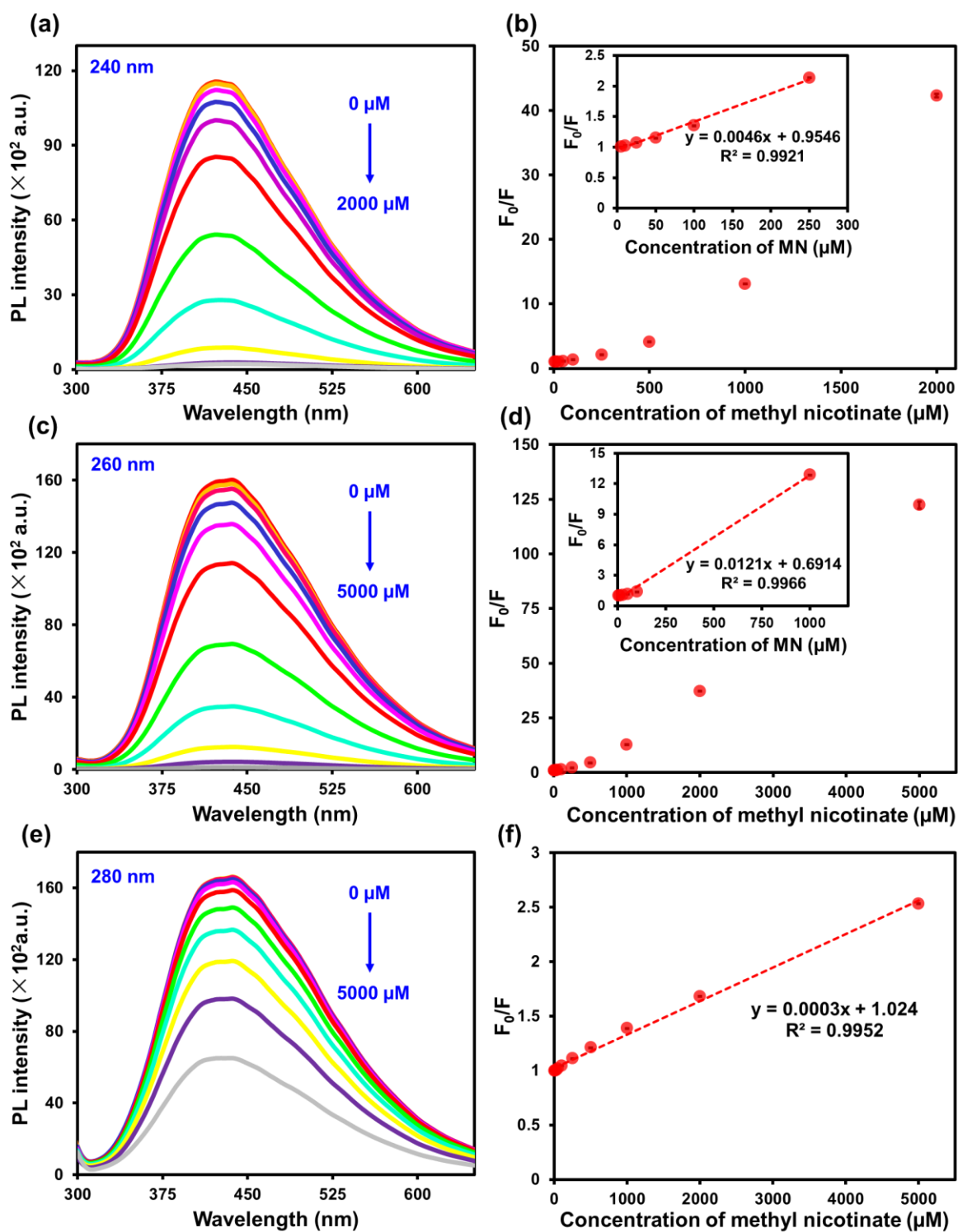


Figure S6. (a, c, e) Fluorescence emission spectra of carbon dots (0.10 mg·mL⁻¹) in the presence of different concentrations of MN at pH 7 with different excitation wavelengths. (b, d, f) The plot between F_0/F and concentrations of MN; inset figure shows the linear range of the plot.

Reference

1. M. Pacquiao, M. D. De Luna, N. Thongsai, S. Kladsomboon and P. Paoprasert, *Highly fluorescent carbon dots from enokitake mushroom as multi-faceted optical nanomaterials for Cr⁶⁺ and VOC detection and imaging applications*, 2018.
2. S. Moonrinta, B. Kwon, I. In, S. Kladsomboon, W. Sajomsang and P. Paoprasert, *Opt. Mater.*, 2018, **81**, 93-101.